contrast to the unstable subcritical bifurcations that occur in plane parallel shear flows in the absence of rotation.

For plane Couette flow and pipe flow, theoretical studies have not found evidence for bifurcation at finite values of *Re*. Nevertheless, the belief in the existence of relatively simple solutions describing states of fluid flow distinct from the basic states of plane Couette flow or pipe flow has persisted. These solutions must be expected to be unstable; therefore, numerical methods are usually not capable of producing them, just as experiments do not exhibit them.

One way of accessing these solutions is by considering the plane Couette or pipe flow problem as a special case of a more general problem, with an additional parameter as a function of which instabilities or bifurcations can be found. The desired solutions are searched by following one or the other of the bifurcating solution branches through secondary bifurcations. For plane Couette flow, the small-gap limit of circular Couette flow provides such an additional parameter in the form of the mean rate of rotation (*7*), which vanishes only in the special case of plane Couette flow. Alternatively, one may consider plane Couette flow between horizontal plates, the lower of which is heated, and the upper of which is cooled. The basic state of flow is not changed by this procedure, but additional instabilities driven by thermal buoyancy become available (*8*). Or an artificial forcing can be applied to gain a point of bifurcation from which a solution branch can be followed to the place of vanishing forcing (*9*). This method has been applied to the case of pipe flow (*10*, *11*).

With these methods, steady solutions are obtained for plane Couette flow and traveling wave solutions for pipe flow. These "tertiary solutions" are separated from the basic states by two bifurcations. They are thus characterized by two wave numbers, in the streamwise and in the transverse directions.

A dominant component of the tertiary solutions are the roll-like eddies with axes parallel to the mean flow. These rolls redistribute momentum and tend to flatten the profile of the mean flow. As a result, the slope of the profile close to the solid boundary steepens, thereby increasing viscous stress. To obtain the same mass flux through the pipe as in the laminar case, a higher pressure gradient is thus needed. Similarly, in the plane Couette case, a stronger force must be applied to keep the plates moving relative to each other with velocity U.

The two-dimensional roll-like eddies would decay if they were not sustained by the three-dimensional components of the tertiary solutions. Streamwise oriented roll-like structures or "streaks" are commonly observed in wall-bounded turbulent shear flows, but the relationship to the tertiary solutions is tenuous at best. There has been little hope to observe the latter solutions in the laboratory because they are almost always unstable.

It thus came as a surprise when Hof *et al.* (*1*) observed the predicted patterns of tertiary solutions in their experiments. Using special disturbances in carefully prepared pipe flow (*12*) and sophisticated visualization techniques, they demonstrate that the tertiary solutions can be realized at least as a transient phenomenon. They find surprisingly close agreement between experimentally observed structures and their theoretical counterparts (*1*).

The puzzle of the visibility of unstable solutions may be explained as follows. The changing state of fluid flow can be considered as a trajectory in the high-dimensional solution space of the basic equations of motion. The tertiary solutions (and the more complex ones bifurcating from them) are unstable in particular directions, but they attract trajectories from most other directions. The trajectories therefore spend much of their time in the neighborhood of those solutions before they are ejected. These solutions may thus be regarded as virtual traffic arteries, which become visible as they attract parcels of momentum and transport them for a while until they deliver them to another artery and decay.

The achievement reported by Hof *et al.* (*1*) stems from a collaboration between engineers, physicists, and mathematicians. It opens the door not only to a full understanding of the transition problem, but also to possibilities for influencing and controlling transitions, with far-reaching engineering implications. The new results also demonstrate that it is never too late to attack an old problem, especially if it is done as an interdisciplinary effort.

References and Notes

1. B. Hof *et al.*, *Science* **305**, 1594 (2004).
2. G. H. L. Hagen, *Pogg. Ann.* **46**, 423 (1839).
3. O. Reynolds, *Proc. R. Soc. London A* **35**, 84 (1883).
4. Here the same definition of the Reynolds number is used as for pipe flow except that D now refers to the width of the channel.
5. J. G. M. Eggels *et al.*, *J. Fluid Mech.* **268**, 175 (1994).
6. "Bifurcation" is a mathematical term used when a secondary solution branches from a primary one.
7. M. Nagata, *J. Fluid. Mech.* **217**, 519 (1990).
8. R. M. Clever, F. H. Busse, *J. Fluid Mech.* **234**, 511 (1992).
9. F. Waleffe, *Phys. Rev. Lett.* **81**, 4140 (1998).
10. H. Faisst, B. Eckhardt, *Phys. Rev. Lett.* **91**, 224502 (2003).
11. H. Wedin, R. R. Kerswell, *J. Fluid Mech.* **508**, 333 (2004).
12. Measurement in the same 30-m-long pipe clearly demonstrated the influence of the Earth's rotation on the laminar flow profile (*13*).
13. A. A. Draad, F. T. M. Nieuwstadt, *J. Fluid Mech.* **361**, 297 (1998).

CHEMISTRY

Multidimensional Snapshots of Chemical Dynamics

Albert Stolow and David M. Jonas

Chemical reactions involve the concerted motions of both atoms and electrons as bonds rearrange on the way from reactant to product. Elementary models use a single, one-dimensional (1D) reaction coordinate to describe motion across a transition state separating reactants from products. However, internal molecular motions along other coordinates tend to prevent molecules from following this lowest energy reaction coordinate. These other motions are not mere energetic reservoirs that may aid or deter motion along the reaction coordinate. Rather, they are intimately involved in the complex flow of electronic charge and vibrational energy during reaction. Recent advances in femtosecond (10^{-15} s) laser and detector technologies are enabling a new generation of experiments that provide true multidimensional views of the dynamics of chemical reactions (*1*).

One emerging approach is based on time-resolved diffraction from crystals that have been photochemically excited by a femtosecond pulse of light, allowing multidimensional measurements of the ensuing atomic motions. For example, Moffat (*2*) and Anfinrud and co-workers (*3*) have performed time-resolved crystal diffraction experiments that yield the time-dependent positions of all atoms during a biochemical photoreaction. The reaction is initiated by a 100-picosecond pulse of light and then probed by measuring the diffraction pattern

A. Stolow is at the Steacie Institute for Molecular Sciences, National Research Council Canada, 100 Sussex Drive, Ottawa, Ontario K1A 0R6, Canada. E-mail: albert.stolow@nrc.ca D. M. Jonas is in the Department of Chemistry and Biochemistry, University of Colorado, Boulder, CO 80309, USA. E-mail: david.jonas@colorado.edu

with a delayed x-ray pulse of the same duration. Large-scale structural rearrangements in proteins (such as the side-chain motions in myoglobin upon carbon monoxide undocking) or at surfaces are almost impossible to observe in another way. Nanosecond time resolution reveals several distinct intermediate structures (*2*), with evidence of driven motions at faster time scales (*3*). New instruments that aim for even higher time resolution using either x-ray or electron scattering are being developed by several groups (*4*–*8*).

Femtosecond two-dimensional infrared (2D IR) spectroscopy is being explored as a way to gain information about transient molecular structures in disordered materials. Bredenbeck and Hamm have used transient femtosecond 2D infrared spectra, which are sensitive to distances between the carbonyl groups in peptides (*9*), to monitor the progress of photoinduced peptide folding. To follow peptide folding on a picosecond time scale, an octapeptide is covalently bound to both ends of an azobenzene conformational switch. First, a femtosecond ultraviolet pulse electronically excites the azobenzene molecule and induces isomerization from the cis to the trans form, triggering the folding of the peptide backbone into its new equilibrium conformation. The time evolution of the azobenzene electronic spectrum, observed in a conventional pump-probe experiment, monitors peptide folding indirectly, because the unfolded peptide inhibits complete isomerization of the switch (*10*). In the new experiments, the femtosecond 2D infrared spectra are sensitive to distances between the carbonyl groups in the peptide itself.

The 2D infrared spectra are recorded by hitting the peptide with a "single-frequency" infrared excitation pulse and then detecting changes in the frequency-resolved infrared absorption spectrum as a function of the initial infrared excitation frequency. When two carbonyl groups in the peptide are within about 0.3 nm, their vibrations are coupled so that excitation of either one measurably shifts the absorption frequency of the other, producing a cross-peak in the 2D spectrum. This is analogous to how the coupling between spins produces cross-peaks in 2D nuclear magnetic resonance (NMR) (*11*, *12*).

Although 2D infrared spectroscopy has a much faster time scale than 2D NMR (*10*), vibrational transitions also have larger linewidths. In the octapeptide, the number of carbonyl groups prevents the resolution of individual cross-peaks. Peptide dynamics were therefore probed only through the overall 2D line shape (see the figure), which changes rather dramatically and continues to change even after the infrared spectrum of the peptide and electronic spectrum of the azobenzene have relaxed to equilibrium. The reduction in the homogeneous linewidth of the 2D infrared spectrum has been interpreted as reflecting more restricted conformational fluctuations around the minimum free energy folded conformation.

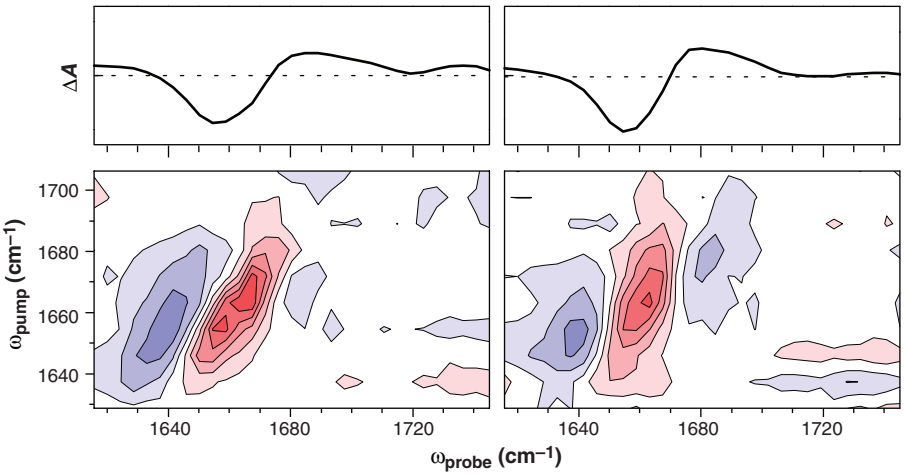

Tracking complex reactions. Polypeptide conformational dynamics observed via transient changes in the 1D (**top**) and 2D IR spectra (**bottom**) of an octapeptide as a function of pump frequency (ω_{pump}) and probe frequency (ω_{probe}). The spectra show differences between the spectra of the intermediates and the reactants at 20 ps (left) and 1.7 ns (right) after cis-trans photoisomerization of the azobenzene bound to both ends of the octapeptide. Blue indicates that the UV photoisomerization pulse and IR pump pulse reduce IR probe absorption, whereas red indicates increased IR probe absorption. While the 1D spectra apparently cease to evolve beyond 20 ps, the 2D spectra continue to reveal changes caused by peptide folding for more than 200 ps. [Data from (*9*)].

A third approach, sensitive to both electronic and atomic motions, is based on photoionization. This approach applies in the gas phase and on surfaces. Because ionization techniques are sensitive to electronic structure and require only that the photon energy exceed the ionization potential, time-resolved photoelectron spectroscopy (*13*–*15*) has been used to probe the coupled redistribution of charge and energy in gas-phase photochemical reactions all the way from reactants to products. Hayden and co-workers have combined time-resolved photoelectron spectroscopy with new coincidence and imaging techniques in "coincidence-imaging spectroscopy" (CIS) (*1*). As a result of developments in charged-particle detector technology, miniaturized versions of the "crossed wire" detector famous in particle physics now allow 3D measurements of a single particle emitted from a chemical event (*16*). The CIS technique measures the energy and 3D angular distributions of ions and electrons in coincidence and as a function of time, thus removing orientational and product channel averaging (*17*). This is important because chemistry occurs in the randomly oriented frame of the molecule, whereas measurements are made in the frame of the laboratory, leading to a loss of information.

In the experiments of Hayden and co-workers, a femtosecond pump pulse initiates a photodissociation reaction, a delayed probe laser pulse ionizes the reacting molecule, and a pair of 3D particle detectors measures the emitted positive ion and electron from a single molecular dissociation/ionization event in coincidence, building up sets of "coincidence maps" that reveal detailed correlations. Because the ion recoil distributions relate to the molecular orientation, the correlated electron distributions reveal details of both charge and energy flow in the reacting molecule. In the photodissociation of the atmospherically important nitrogen dioxide molecule ($NO_2 \rightarrow NO + O$), CIS was used to directly observe the evolving rearrangement of the electron cloud (*1*) on the NO molecule as its O atom partner breaks its bond and leaves (*17*).

The elucidation of complex chemical processes rests on the availability of femtosecond laser sources. To do the same for correlated electron dynamics of strongly bound electrons requires pulses that are 1000 times as fast—that is, attosecond (10^{-18} s) pulses. Attosecond pulses have been demonstrated, and a new approach to time-resolved electron dynamics has been reported by Krausz and co-workers (*18*). In an alternate approach, attosecond measurements based on correlation techniques in a strong laser field were reported by Corkum and co-workers (*19*). These first results open up yet another frontier for the time-resolved measurement of the ultrafast processes that occur during chemical reactions.

References and Notes

1. Many of these approaches were recently discussed in the symposium on *Emerging Ultrafast* Spectroscopies: From Chemistry to Biophysics, 227th National Meeting of the American Chemical Society, Anaheim, CA, 28 March to 1 April 2004.
2. K. Moffat, *Faraday Discuss.* **122**, 65 (2003).
3. F. Schotte *et al.*, *Science* **300**, 1944 (2003).
4. F. Benesch, T. Lee, Y. Jiang, C. G. Rose-Petruck, *Opt. Lett.* **29**, 1028 (2004).
5. M. F. Decamp *et al.*, *Phys. Rev. Lett.* **91**, 165502 (2003).
6. S. L. Johnson *et al.*, *Phys. Rev. Lett.* **91**, 157403 (2003).
7. B. J. Siwick, J. R. Dwyer, R. E. Jordan, R. J. D. Miller, *Science* **302**, 1382 (2003).
8. C. Y. Ruan *et al.*, *Proc. Natl. Acad. Sci. U.S.A.* **101**, 1123 (2004).
9. J. Bredenbeck *et al.*, *J. Phys. Chem. B* **107**, 8654 (2003).
10. S. Spörlein *et al.*, *Proc. Natl. Acad. Sci. U.S.A.* **99**, 7998 (2002).
11. D. M. Jonas, *Science* **300**, 1515 (2003).
12. D. M. Jonas, *Annu. Rev. Phys. Chem.* **54**, 425 (2003).
13. V. Blanchet, M. Zgierski, T. Seidemann, A. Stolow, *Nature* **401**, 52 (1999).
14. A. Stolow, A. E. Bragg, D. M. Neumark, *Chem. Rev.* **104**, 1719 (2004).
15. L. Lehr *et al.*, *Science* **284**, 635 (1999).
16. K. A. Hanold, M. C. Ganer, A. E. Continetti *Phys. Rev. Lett.* **77**, 3335 (1996).
17. J. A. Davies, R. E. Continetti, D. W. Chandler, C. C. Hayden, *Phys. Rev. Lett.* **84**, 5983 (2000).
18. R. Kienberger *et al.*, *Nature* **427**, 817 (2004).
19. H. Niikura *et al.*, *Nature* **421**, 826 (2003).

MICROBIOLOGY

Pathogenic Bacteria Prefer Heme

Tracey A. Rouault

Almost all cells and organisms require iron to facilitate basic cellular processes such as respiration and DNA biosynthesis. Diverse and complex iron-uptake systems have evolved throughout the biological world to provide iron for numerous proteins, particularly those involved in energy capture and oxygen transport. Indeed, in parts of the great oceans, a complete lack of iron profoundly limits bacterial growth (*1*, *2*). In most environments, however, iron uptake is limited not by its absence, but by the fact that it is insoluble and inaccessible. To facilitate iron uptake, free-living bacteria and fungi have adopted several strategies. Some secrete compounds known as siderophores that solubilize and bind to an external source of iron with high affinity; the iron-siderophore complexes are then imported into the bacteria by specific transporter proteins. Others have uptake systems that import free iron salts directly (*3*, *4*). To combat microbial infections, animals strictly limit the availability of free iron in their blood and tissues. They do this by ensuring that iron in blood and secretions is carried by the high-affinity iron-binding proteins transferrin and lactoferrin, which create a primary line of defense against infection termed the "iron blockade" (*5*). The two ferric iron-binding sites of transferrin are rarely fully saturated, and an excess of unsaturated transferrin (apo-transferrin) ensures that free iron is virtually eliminated from blood. Pathogenic microorganisms, therefore, must overcome major obstacles if they are to acquire iron and thrive in their animal hosts. On page 1626 of this issue, Skaar and colleagues (*6*) explore how the pathogenic bacterium *Staphylococcus aureus* acquires the iron that it needs for growth in two different animal hosts. By growing the bacteria in the presence of the two principal iron sources found in mammals—diferric transferrin and the iron-porphyrin heme—the investigators show that most of the iron taken up by *S. aureus* during the initial phases of infection is obtained from heme.

Enhanced online at www.sciencemag.org/cgi/content/full/305/5690/1577

Although most bacteria are unable to grow in media in which the only iron sources are transferrin-iron and heme, some bacteria have developed strategies that enable them to obtain iron from these two sources (*7*, *8*). To determine whether *S. aureus* prefers transferrin-iron or heme as a source of iron, Skaar and colleagues labeled heme with ^{54}Fe and transferrin with ^{57}Fe, two rare and stable iron isotopes (*9*). After establishing that *S. aureus* grew well in medium supplemented with equimolar amounts of ^{54}Fe heme and ^{57}Fe transferrin, they analyzed the isotope content of cells using inductively coupled plasma–mass spectrometry (ICP-MS) at various times during growth. They discovered that *S. aureus* markedly prefers a source of iron derived from heme. Analysis of the *S. aureus* genome revealed that it encodes seven putative membrane transporter proteins that have some homology to known bacterial iron transporters. Using mutational inactivation and ICP-MS to monitor uptake of heme iron, the investigators identified a heme transport system in *S. aureus* composed of three genes

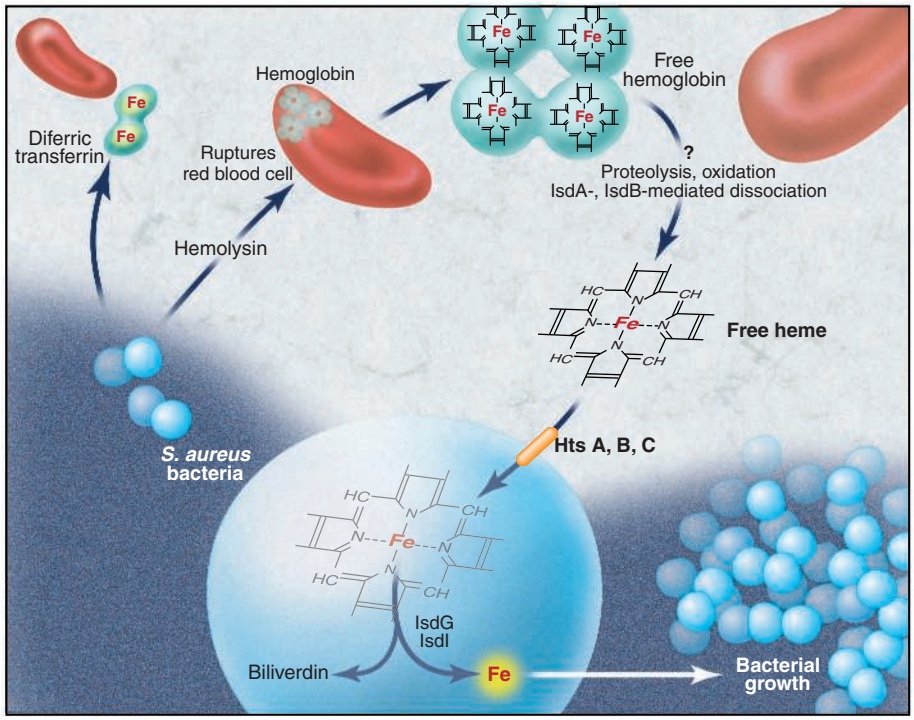

Bloodletting explained. *S. aureus* bacteria obtain most of the iron (Fe) that they need for growth in mammalian hosts from an iron-containing porphyrin ring called heme. *S. aureus* produces hemolysins that lyse red blood cells containing heme in the form of hemoglobin. It is unclear how the bacteria break down the released hemoglobin to heme, but the bacterial enzymes IsdA and IsdB may be involved. The bacteria then import heme via transporter proteins encoded by the *hts* ABC operon. The heme is then catabolized by the heme oxygenase-like enzymes, IsdG and IsdI, with the release of iron and biliverdin (a breakdown product of the porphyrin ring). The free iron released from heme is used to fuel further bacterial growth. The practice of bloodletting in the pre-antibiotic era may have been an attempt to starve pathogenic bacteria of the iron that they need for growth.

CREDIT: KATHARINE SUTLIFF/*SCIENCE*

The author is in the Section on Human Iron Metabolism, Cell Biology and Metabolism Branch, the National Institute of Child Health and Human Development, National Institutes of Health, Bethesda, MD 20892, USA. E-mail: trou@helix.nih.gov

ERRATUM

post date 13 September 2004

Owing to an error at *Science*, an incorrect version of this PDF, containing typographical errors, was posted when the article was first published (the print and full-text HTML versions of the article, however, are correct). The current version of the PDF corrects the errors in that original version.